Journal of South American Earth Sciences 59 (2015) 19–26

Contents lists available at ScienceDirect

Journal of South American Earth Sciences

journal homepage: www.elsevier.com/locate/jsames

Recent trends on glacier area retreat over the group of Nevados Caullaraju-Pastoruri (Cordillera Blanca, Peru) using Landsat imagery

Claudio Durán-Alarcón [a], Caroline M. Gevaert [b, g], Cristian Mattar [a, *], Juan C. Jiménez-Muñoz [b], José J. Pasapera-Gonzales [c], José A. Sobrino [b], Yamina Silvia-Vidal [d], Octavio Fashé-Raymundo [e], Tulio W. Chavez-Espiritu [f], Nelson Santillan-Portilla [f]

[a] Laboratory for Analysis of the Biosphere, Dpt. of Environmental Sciences and Renewable Natural Resources, University of Chile, Av. Santa Rosa 11315, La Pintana, Santiago, Chile
[b] Global Change Unit, Image Processing Laboratory, University of Valencia Science Park, C/Catedrático José Beltrán 2, 46980 Paterna, Valencia, Spain
[c] Comisión Nacional de Investigación y Desarrollo Aeroespacial (CONIDA), Agencia Espacial del Perú, Av. Luis Felipe Villarán 1069, San Isidro, Lima 27, Peru
[d] Instituto Geofísico del Perú, Calle Badajoz N° 169, Mayorazgo IV Etapa, Ate Vitarte, Lima, Peru
[e] Laboratorio de Física Ambiental, Facultad de Ciencias Físicas, Universidad Nacional Mayor de San Marcos (UNMSM), Calle Germán Amézaga N° 375, Lima, Peru
[f] Unidad de glaciología, Autoridad Nacional del Agua (ANA), Calle Diecisiete N° 355, Urb El Palomar, San Isidro, Lima, Peru
[g] Department of Earth Observation Science, University of Twente, 7500 AE Enschede, The Netherlands

ARTICLE INFO

Article history:
Received 13 July 2014
Accepted 26 January 2015
Available online 3 February 2015

Keywords:
Glacier
Caullaraju-Pastoruri
Cordillera Blanca
Landsat
NDSI
LST

ABSTRACT

The Cordillera Blanca, located in the central zone of the Andes Mountains in Peru, has shown a retreat in its glaciers. This paper presents a trend analysis of the glacier area over the groups of Nevados Caullaraju-Pastoruri from 1975 to 2010 using Landsat-5 Thematic Mapper (TM) imagery. In the case of the Nevados Pastoruri/Tuco, the study period was extended back to 1957 by using an aerial photograph taken that year. The extent of clean glacier ice was estimated using Normalized Difference Snow Index (NDSI) thresholds. Moreover, the estimation of debris-covered glacier ice was retrieved by means of a decision tree classification method using NDSI, Normalized Difference Vegetation Index (NDVI) and Land Surface Temperature (LST). Area estimations derived from Landsat imagery were compared to the glacier ground-truth data in 1975 and 2010. Results show a statistically significant ($p < 0.05$) decreasing trend over the whole study area. Total glacier area decreased at a rate of 4.5 km^2 per decade from 1975 to 2010, with a total loss of 22.5 km^2 (58%). Lower decreasing rates were found for the period 1987–2010: 3.5 km^2 per decade with a total loss of 7.7 km^2 (32.5%). In the case of the Nevados Pastoruri/Tuco, decreasing rates of clean ice extent were constant for the periods 1957–2010, 1975–2010 and 1987–2010, with values close to 1.4 km^2 per decade and a total loss between 1957 and 2010 estimated at about 5 km^2 (54%). This work shows an evident area decrease in the Caullaraju-Pastoruri tropical glaciers, which needs to be included in a future hydrological scenario of local adaptability and water management.

1. Introduction

The Cordillera Blanca (8°30′ – 10°10′S) is one of the most important areas in the Peruvian Andes mountains, where tropical glaciers have experienced several retreats. These Peruvian glaciers have been studied in the tropical Andes and make-up the world's most extensively glacier-covered tropical mountain range (Vuille et al., 2008a; Jomelli et al., 2009). The retreat in the entire Cordillera Blanca was estimated at a loss of 161 km^2 or 25% of their area relative to 1987 (Burns and Nolin, 2014) in addition to a significant retreat overall since the Little Ice Age Maximum (LIAM) (Vuille et al., 2008a).

The glacier retreat observed in this mountain range during the 20th century was substantial and has been documented in many studies (Vuille et al., 2008b and references therein). The general retreat has not been uniform, glacier retreat and advance alternating at different time periods: major advances occurred in the

* Corresponding author.
E-mail addresses: claudioduran@ug.uchile.cl (C. Durán-Alarcón), cmattar@uchile.cl (C. Mattar).

http://dx.doi.org/10.1016/j.jsames.2015.01.006
0895-9811/

1920s, drastic recession in the 1930s and 1940s, almost constant extent during the two following decades with a slight advance in the 1970s, and an accelerated retreat since the 1980s, though with recent advances in some glaciers (Solomina et al., 2007).

Changes in glacier area typically affect runoff and water storage in the tropical catchment (Juen et al., 2007). Glaciers in this region act as temporal water storage for precipitation falling as snow at high elevation in the wet season from about October to April (Schauwecker et al., 2014). Part of the stored water is released during the dry season, compensating for the scarce number of precipitation events between May and September (Kaser et al., 2003).

To monitor tropical glaciers, several different techniques have been used to estimate the clean ice glacier area and its trend, one of which is remote sensing. Several works have used optical remote sensing to assess the spatial and temporal patterns of tropical glacier retreats (Klein and Isacks, 1999; Silverio and Jaquet, 2005; Kaser and Osmaston, 2001; Racoviteanu et al., 2008 a,b; Burns and Nolin. 2014; López-Moreno et al., 2014). Despite the fact that the presence of clouds in the acquired scene partly limits the use of optical imagery, the availability of a number of medium/high resolution sensors (~1–100 m) from the 1970s allows for the multitemporal analysis of the glacier area changes. In this sense, the recent availability of the Landsat historical archive is especially important because it provides data at spatial resolutions ranging between 15 and 120 m covering the Visible and Near-InfraRed (VNIR), Short-Wave InfraRed (SWIR) and Thermal InfraRed (TIR) regions of the electromagnetic spectrum.

Most studies based on Landsat imagery over the Cordillera Blanca use a threshold of the Normalized Snow Difference Index (NSDI) and post-processing techniques to delimitate glaciers area (Silverio and Jaquet, 2005; López-Moreno et al., 2014; Burns and Nolin, 2014). Nevertheless, the use of Land Surface Temperature (LST) and the Normalized Vegetation Difference index (NDVI) can complement the delineation of the glacier area by using a semi-automatic approach. Thus, the aim of this work is to present a single, semi-automatic method to assess the clean ice glacier and also to analyze the spatial and temporal patterns by using long term data based on aerial photography and Landsat historical imagery over the group of Nevados Caullaraju-Pastoruri (Cordillera Blanca, Peru), using a combination of NDSI, NDVI and LST data. The structure of this manuscript is detailed as follows: Section 2 describes the study area, remote sensing data and meteorological information. Section 3 presents the method used to perform an approximate clean ice glacier and debris-covered identification. Sections 4 and 5 show the results and discussion, respectively. Finally, the conclusions are presented in Section 6.

2. Study area and data set

2.1. The Caullaraju-Pastoruri Nevados

The study area selected for this work belongs to the glaciated area encompassing the following groups of Nevados (from west to east): Caullaraju, Jenhuaracra, Condorjitanca, Huiscu, Tuco and Pastoruri, located in the southeast part of the Cordillera Blanca. It also includes the two small Nevados of (from north to south) Santon and Rajutuna (Fig. 1). Hereinafter, this area will be referred as the Caullarju group of Nevados. The altitude above sea level (a.s.l.) of the study area is higher than 5000 m (the maximum altitude in the Nevado Caullaraju is ≈5682 m a.s.l., and the maximum altitude in the Nevado Pastoruri is ≈5200 m a.s.l.). The group of Nevados is located in the Cátac district of the province of Recuay (Department of Ancash, Region of Ancash, Peru), to the east of the Santa River, and it is located inside Huascarán National Park.

2.2. Landsat imagery

The Landsat images were acquired from the U.S. Geological Survey's Earth–Explorer interface. L5/TM images covered the period 1987–2010, though the study period was extended back to 1975 by using one L2/MSS image (Table 1). Over the Nevado Pastoruri, the study period was extended back to 1957 using one orthorectified aerial photograph taken during that year. Landsat imagery acquired between May and September was selected for this study, since this time period is considered to be the dry season, when runoff is almost exclusively due to glacier melting and temporal snow is minimized (Kaser et al., 2003). Final selection of the imagery was supported by visual inspection over the area. Selected images were free of clouds, so additional cloud masking was not required.

2.3. Ancillary information

In order to analyze the longest time period possible, an aerial photograph taken in 1957 was used in this work. This aerial photograph was orthorectified by using ground control points and tie points. A Digital Elevation Model (DEM) was used in the identification of debris-covered glacier areas. The DEM was provided by the *Instituto Geográfico Nacional del Perú*, and it was geo-referenced from interpolation of contour lines at 15 m spatial resolution.

Meteorological data was also used in this work. Precipitation data from the Milpo meteorological station, located approximately 2 km from the study area (Fig. 1), was analyzed in order to verify the lack of precipitation during the week preceding the image acquisition date, thus avoiding the presence of temporal snow.

Finally, ground truth vectors delineating glacial extension in 1970 and 2010 were used to test the results extracted from the satellite images. These vectors were constructed following the Global Land Ice Measurements from Space (GLIMS) project guidelines (Raup et al., 2007) and they were provided by the Peruvian institution *Autoridad Nacional del Agua* (ANA). Total glacier areas extracted from the ground-truth vectors were 32.02 km^2 in 1970 and 18.69 km^2 in 2010.

3. Method

3.1. Landsat imagery processing

The Landsat imagery used in this work included a Level 1T processing (terrain correction product) with systematic radiometric and geometric accuracy corrections derived from data collected by the sensor and spacecraft, and topographic correction using a Digital Elevation Model (DEM) based on the Global Land Survey 2000 (GLS2000). Each image was visually inspected to select images with very low cloud cover. Visual inspection and analysis of precipitation data were also used to confirm the lack of temporal snow over the area. Finally, seven Landsat images were used in the temporal analysis (Table 1).

Conversion from Digital Counts to at-sensor radiance (all bands), Top of Atmosphere (TOA) reflectances (only VNIR/SWIR bands) and at-sensor brightness temperature (only TIR bands) was performed following the well-known procedure presented in Chander and Markham (2003) and the subsequent updates provided in Chander et al. (2007, 2009).

Atmospheric correction was performed to both VNIR/SWIR and TIR bands to retrieve respectively at-surface reflectances and Land Surface Temperature (LST). In the case of VNIR/SWIR bands, at-surface reflectances were obtained using a simple atmospheric correction method based on the Dark Object Subtract (DOS), as described in Chavez (1996). LST was retrieved from TIR data using the Single-Channel (SC) algorithm revised in Jiménez-Muñoz et al.

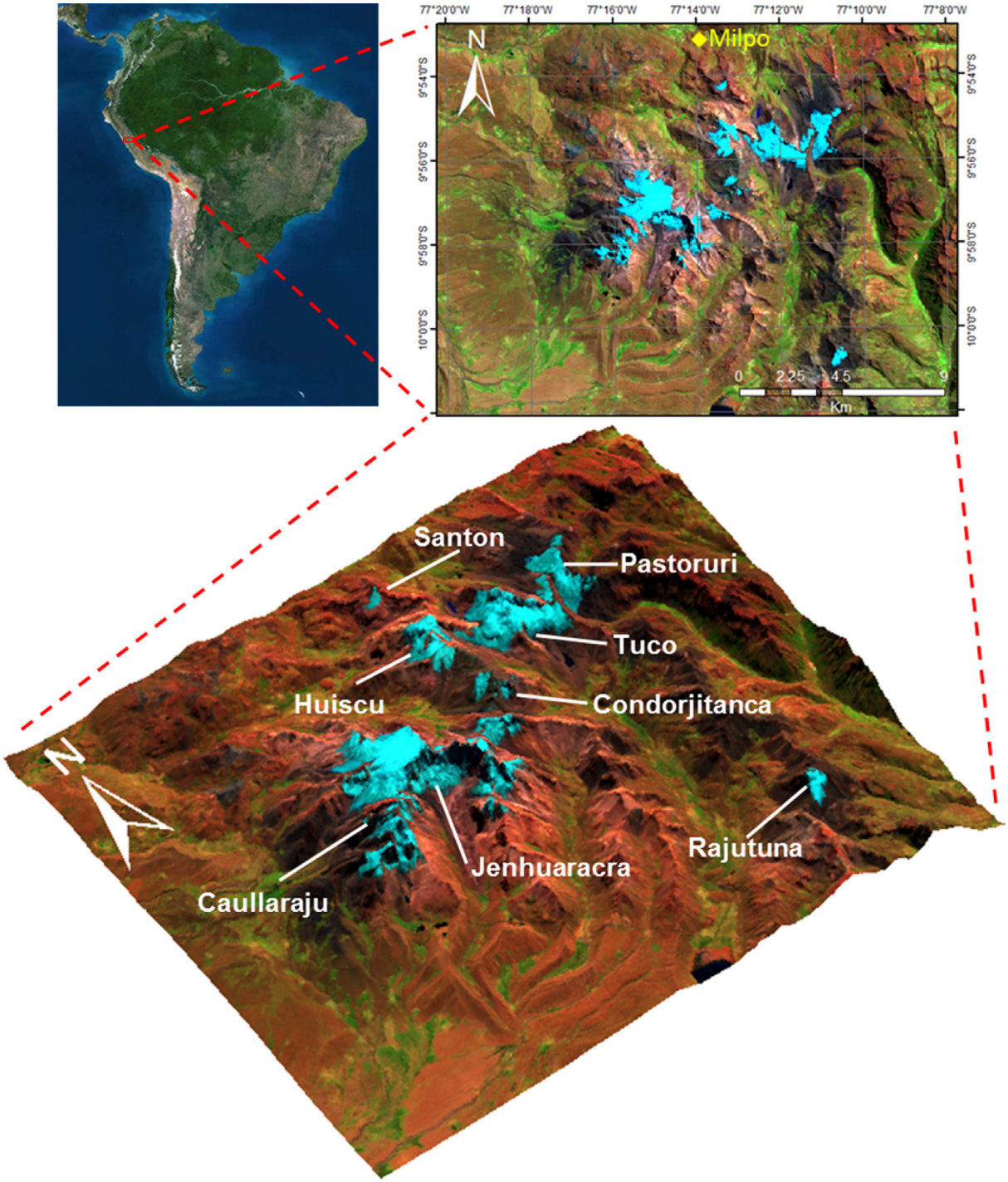

Fig. 1. Nevados of Caullaraju – Pastoruri and nearest glaciers. The location of the Milpo meteorological station is also indicated.

(2009). Surface emissivity, a required input to the SC algorithm, was estimated using the simplified NDVI Thresholds Method (Sobrino et al., 2008) over soil and vegetated pixels, and by assignation of fixed values to ice/snow, water and debris-covered pixels. Selection of emissivity values was performed by analysis of samples included in the ASTER spectral library (Baldridge et al., 2009). Spectral values were averaged using sensor Spectral Response Function (SRF): a value of 0.99 was selected for green vegetation and water, a value of 0.97 for ice/snow, and a value of 0.98 for debris-covered surfaces. This last value was obtained as a mean value for different sedimentary rocks included in the spectral library.

3.2. Glacier area estimation

3.2.1. Clean ice identification

Delineation of clean ice glacier can be achieved in a robust and time effective way by thresholding single band ratio images or normalized indices, which also allows for the identification of snow/ice in shadows. Automatic identification of glacier area using these techniques is based on the high albedo of snow/ice in the VNIR and medium to low albedo in the SWIR (Dozier, 1989). For instance, band ratio TM3/TM5 has been used to report a glacier inventory for the Canadian Mountains (Bolch et al., 2010), Norway

Table 1
Final selection of Landsat imagery used in this study. All images were acquired during the dry season (May to September) and precipitation was not registered at least one week before the acquisition. Cloud contamination was not observed over the study area.

Date	Sensor
1975-08-04	L2/MSS
1987-05-31	L5/TM
1995-06-06	L5/TM
1997-06-27	L5/TM
1998-07-16	L5/TM
2005-06-17	L5/TM
2010-08-18	L5/TM

(Andreassen et al., 2008), and the western Himalaya (Frey et al., 2012). The band ratio TM4/TM5 has also proved useful for glacier delineation in various Alpine studies (Paul et al., 2002, 2004a). Normalized indices, such as the Normalized Difference Snow Index (NDSI), have been successfully applied to the Cordillera Blanca (Silvero and Jaquet, 2005; Racoviteanu et al., 2008a) and other areas, such as the Eastern Himalaya (Racoviteanu and Williams, 2012). A complete review of methods for analyzing glacier characteristics from optical remote sensing data can be found in Racoviteanu et al. (2008b). In this study, the NDSI was selected to identify clean ice areas and was computed from L5/TM bands 2 and 5 (using at-surface reflectance values):

$$NDSI = \frac{TM2 - TM5}{TM2 + TM5} \quad (1)$$

Once the NDSI was computed, a threshold was chosen to discriminate clean ice from the surrounding area. NDSI thresholds between 0.4 and 0.6 were found to be optimal in previous studies (Racoviteanu et al., 2008a), although other studies used automatic thresholding methods to determine optimal values (Yin et al., 2013). We found an optimal NDSI threshold value of 0.5. After the NDSI thresholding, a 3x3 majority filter was applied to the glaciated area to remove isolated non-glacial snow pixels and fill small voids, such as those due to rock outcrops in glacier ice, as suggested by Andreassen et al. (2008).

In the case of the L2/MSS image, bands are not appropiate for computing the NDSI, so a supervised classification (maximum likelihood classification rule) was performed to identify clean ice areas using digital counts as input data.

3.2.2. Identification of debris-covered glacier areas

Clean ice glaciers are often partly covered by surface debris, which hampers the identification of glacier area when using the same NDSI threshold as the one used to identify clean ice. Strategies for supraglacial debris satellite mapping remain in development, although multispectral thermal approaches to map geologic composition of glacier debris are promising (Casey et al., 2012). Due to the limitations of the Landsat spectral configuration (only 1 TIR band in the case of L5/TM), we will focus on debris-covered glacier identification using decision trees and multisource data. The method used in this study was based on the one presented in Paul et al. (2004b), with a number of alterations. The following procedure was followed:

i. Clean glacier ice was determined by identifying pixels with a NDSI>0.5.
ii. Vegetated areas were identified as those having an NDVI > 0.2, rather than using the hue component of an intensity-hue-saturation transformation;
iii. the slope criterion was unaltered: slopes were obtained from the DEM and those steeper than 24° were defined as too steep for glaciers (Paul et al., 2004b);
iv. a temperature criterion was added, taking advantage of the lower temperature of debris-covered ice relative to the surrounding slopes. To allow for scene-dependent temperature (LST) variations, this threshold was empirically defined as areas colder than the average scene temperature (LST_{μ}) minus the standard deviation (LST_{σ});
v. debris-covered glaciers were thus identified as those having an NDSI<0.5 (not clean-ice), NDSI < 0.1 (not vegetation), slope < 24, and LST < LST_{μ}-LST_{σ}.
vi. after applying the four criteria, a 3x3 majority filter was applied to remove isolated pixels. Then, glaciated areas with an area of less than 0.001 km^2 and debris-covered ice with no bordering clean-ice pixels were eliminated.

In the case of the L2/MSS image, the method used to estimate debris-covered areas was modified, since the spectral configuration of the MSS sensor does not allow for the computation of the NDSI and LST. Instead, the supervised classification was used to identify clean snow and vegetated areas (replacing the NDSI and NDVI parameters, respectively). The remaining areas were combined with the slope factor described above to delimit possible debris-covered ice. There was no suitable substitute available for the LST parameter, so this factor was not included in the analysis. Due to band configuration limitations, results extracted from the MSS image are expected to be less accurate than those extracted from the TM images.

3.2.3. Water mask

NDSI values over water bodies are usually high, so glacier area estimations from NDSI values can be overestimated if water bodies are present in the study area. Note that different lakes can form near the glacier area due to ice melting, so it is necessary to apply a water mask prior to the area computation. Although some band thresholds could be used to identify water bodies in the study area, visual inspection of RGB compositions and a priori knowledge of the site produced better results. The water mask was applied to both the clean ice glacier and the debris-covered glacier areas.

3.3. Trend analysis

The sign of the trend estimated for the glacier area (increase or decrease) and its significance were obtained from a Mann-Kendall analysis, a non-parametric method that makes no assumption on distribution of data (Kendall, 1975). The slope or magnitude of the trend was estimated using Sen's method (Sen, 1968), which also provides upper and lower limits of the slope at a certain confidence level. As a general rule, trends were considered significant when p-level<0.05 (confidence level 95%, $\alpha = 0.05$). For comparison, a simple linear regression was also used to compute the trends.

4. Results

4.1. Maps of surface parameters

The RGB composition (Fig. 1) enhances the clean ice of the glaciated area in the color blue and the surfaces with a high vegetation cover in green. Water bodies have mostly negative NDVI values, so they might be confused with clean ice, which also have negative NDVI values. Clean ice and debris-covered glacier are better detected in the NDSI image, although water bodies cannot be discerned in the NDSI image because of the similar NDSI values between water and clean ice. Moreover, NDSI is for the most part

insensitive to the presence of shadows. In terms of LST, glaciated area is clearly distinguishable from the surrounding area because of its lower temperature (around 270 K). Even debris-covered glacier areas show a different (higher) temperature from that of clean ice areas. Pixels located in the external contour of the glacier show temperatures >276 K, thus suggesting that these pixels are probably located at the transition from clean ice to debris-covered ice.

4.2. Trends in glacier area

Fig. 2 shows the temporal evolution (1975–2010) of clean ice and total (clean ice + debris-covered) glacier area over the whole study area. Results are compared to the total glacier area estimated from the ground-truth data in years 1970 and 2010. Values extracted from both Landsat imagery and ground-truth data show a clear decreasing trend. The total area lost from 1970 to 2010 according to the ground-truth data was 13.3 km^2, almost 42% of the glacier area in 1970. Results are consistent when compared to decreases in clean ice area estimated from Landsat imagery, with a total loss from 1975 to 2010 of 15.9 km^2. However, significant discrepancies are observed when ground-truth data are compared to total glacier area extracted from the Landsat imagery, since in this case the total area lost from 1975 to 2010 is 22.5 km^2 (~58%). This difference may be attributed to the higher uncertainty on debris-covered areas estimated from the limited spectral configuration of Landsat 2/MSS (year 1975). In fact, when changes in glacier area are estimated using only the Landsat 5/TM data (period 1987–2010 in this case), the decreasing rates obtained from the ground-truth data and Landsat imagery are consistent: −0.33, −0.35, and −0.40 km^2/year for ground-truth data, total glacier area from Landsat imagery, and clean ice area from Landsat imagery, respectively. Decreasing rates in glacier area using Mann-Kendall/Sen method over the whole study area are also provided in Table 2. Trends were statistically significant, at least at the 95% confidence level.

Analysis of glacier area trends over particular groups of Nevados was also performed. Temporal evolution of clean ice and total glacier area (1975–2010) for the different groups of Nevados is presented in Fig. 3, while detailed decreasing rates in glacier area are included in Table 2. The spatial pattern of clean ice retreat for the different years is displayed, in Fig. 4 based on aerial photograph, and in Fig. 5 using Landsat imagery. The lowest decreasing rates are obtained for the smallest Nevados (Santon and Rajutuna), whereas the highest rates are obtained for the largest Nevados (Caullaraju & Jenhuaracra, Pastoruri & Tuco). In fact, a significant linear relationship was observed between decreasing area rate and size of the glacier, with R^2 = 0.987. However, the total change over the smallest Nevados was higher than total change over the largest Nevados, and higher than the ice lost over the whole study area.

Regarding the Pastoruri/Tuco subset, the average trend in clean ice extent from 1957 to 2010 is −0.14 km^2/year, which is

Table 2
Trends in clean ice and total glacier area change (km^2/year) over the different groups of Nevados. Slope (slp) values were obtained from linear regression (lin) and using Mann-Kendall/Sen analysis (sen). In this last case, upper and lower values of the slope at the 95% confidence level are given in brackets. Total area change is included in the last two columns, both in terms of absolute change (Δ_{area}) and in relative terms (Δ_{rel}). In all cases, trends were significant at least at the 95% confidence level.

Group of Nevados	Period	Δ_{area} (km^2)	Δ_{rel} (%)
Clean Ice Area			
Santon	1975–2010	−0.64	−85.2
	1987–2010	−0.48	−81.0
Rajutuna	1975–2010	−1.11	−76.4
	1987–2010	−0.59	−63.2
Caullaraju & Jenhuaracra	1975–2010	−7.26	−51.5
	1987–2010	−3.73	−35.3
Condorjitanca & Huiscu	1975–2010	−2.00	−61.1
	1987–2010	−1.14	−47.2
Pastoruri & Tuco	1957–2010	−5.04	−53.6
	1975–2010	−4.84	−52.6
	1987–2010	−3.12	−41.7
All group of nevados	1975–2010	−15.85	−55.1
	1987–2010	−9.05	−41.2
Total Glacier Area			
Santon	1975–2010	−0.68	−68.1
	1987–2010	−0.38	−54.8
Rajutuna	1975–2010	−1.80	−83.1
	1987–2010	−0.64	−63.5
Caullaraju & Jenhuaracra	1975–2010	−8.98	−51.0
	1987–2010	−2.76	−24.2
Condorjitanca & Huiscu	1975–2010	−2.98	−65.5
	1987–2010	−1.13	−42.0
Pastoruri & Tuco	1975–2010	−8.94	−63.4
	1987–2010	−2.82	−35.3
All group of nevados	1975–2010	−22.53	−58.4
	1987–2010	−7.73	−32.5

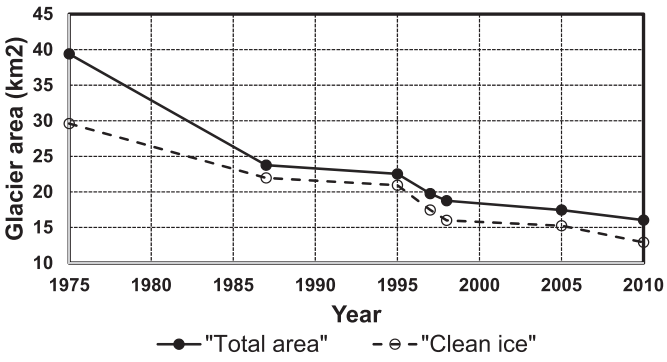

Fig. 2. Clean ice area and total area (clean ice and debris-covered ice) extracted from the different Landsat imagery over the study area (group of Nevados).

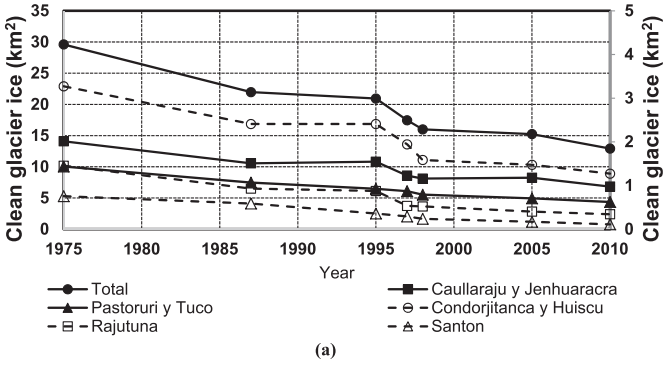

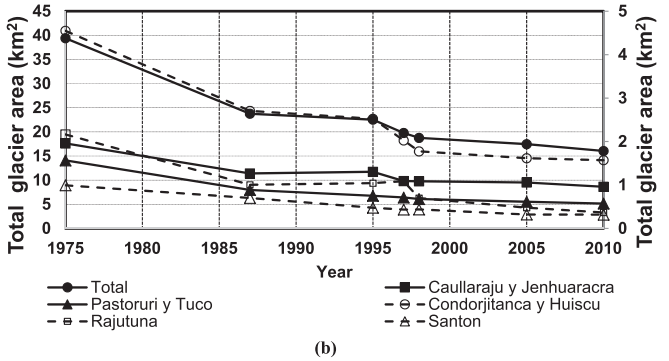

Fig. 3. **(a)** Clean ice area and **(b)** total area (clean ice and debris-covered ice) extracted from the different Landsat imagery over particular groups of Nevados.

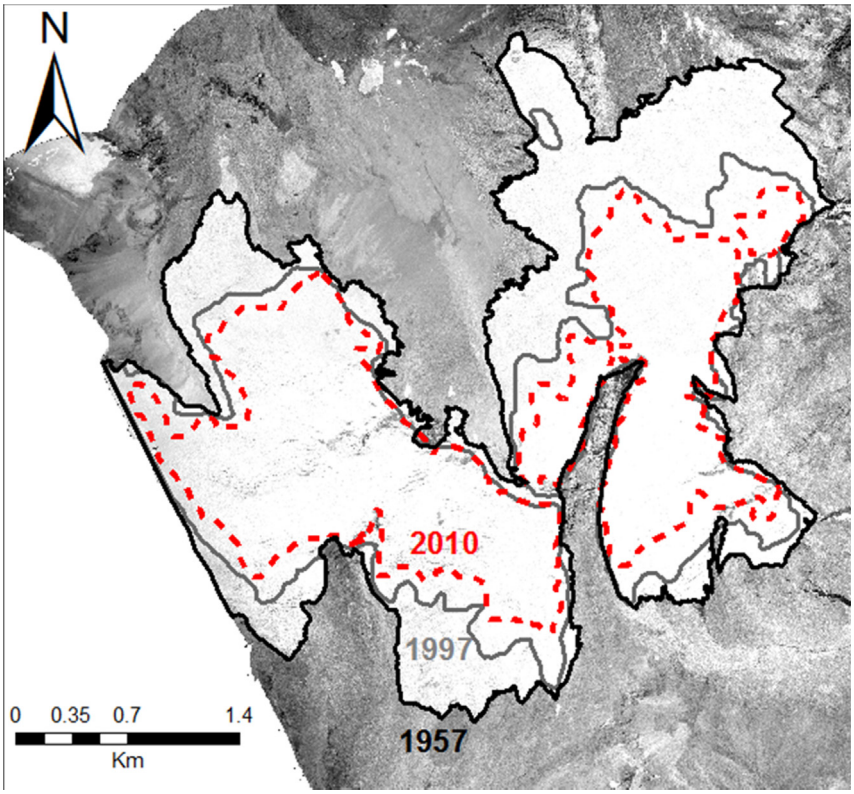

Fig. 4. Spatial patterns in clean ice glacier of Pastoruri/Tuco Nevado between 1957 and 2010. Black, grey and red lines indicate the estimated glacier limits for each year displayed over an aerial photograph acquired in 1954. (For interpretation of the references to colour in this figure legend, the reader is referred to the web version of this article.)

comparable to the trend without the aerial image (1975–2010) and also without the Landsat2/MSS, also −0.14 km^2/year. The clean ice loss of the Pastoruri glacier is 54% from 1957 to 2010, 53% from 1975 to 2010, and 42% from 1987 to 2010, indicating that a glacial retreat of the Pastoruri glacier is similar or slightly lower than that of the entire study area (55% for 1975–2010, and 41% for 1987–2010).

5. Discussion

The historical archive of Landsat imagery is a useful dataset for glacier monitoring at low cost and optimal temporal, spatial and spectral resolution, at least for clean ice identification. To calculate the extent of clean glacier ice, a number of methods were first applied to the 2010 image and compared to the 2010 ground-truth data to identify which method is optimal for the present study area (results not shown in the paper). band ratios (TM4/TM5 and TM3/TM5), normalized indices (NDSI and NDSII), clustering algorithms using raw data and corrected reflectivity values, a supervised Maximum Likelihood Classification, and target detection algorithms were applied. From the mentioned methods, those based on band ratios and normalized indices are the most used ones in glacier delimitation studies (Bolch et al., 2010; Andreassen et al., 2008; Paul et al., 2002; Silvero and Jaquet, 2005; Racoviteanu et al., 2008a; Racoviteanu and Williams, 2012). Nevertheless, the NDSI method was finally selected because it produced good results, it is less sensitive to illumination changes and band ratio methods have proven to have some difficulties in the delimitation of glaciers due to lakes, fresh snow and debris-cover present on the glacier surface (Racoviteanu et al., 2008b). In addition, it was used in previous works regarding glacier area mapping of the Cordillera Blanca (Silvero and Jaquiet, 2005; Burns and Nolin, 2014).

According to Burns and Nolin (2014), atmospheric corrections (added to the topographic corrections) are required to select a single threshold value applicable to a multitemporal series of satellite imagery, although other studies in the Cordillera Blanca used raw data or un-corrected reflectances (e.g. Silverio and Jaquet, 2005). In this study, atmospherically-corrected reflectances were used to select a unique NDSI threshold of 0.5, which worked well for the delineation of clean ice glacier, whereas other thresholds such as 0.4 and 0.6 provided similar area values. Values of NDSI thresholds were supported by analysis of every single NDSI histogram. Contrarily, debris-covered ice identification from NDSI thresholds requires detailed visual inspection and is somewhat arbitrary. We explored the possibility of detecting debris-covered ice by modifying an existing methodology based on decision trees and multisource data (Paul et al., 2004b). The methodology used in this work is based on the inclusion of LST obtained from TIR data (after atmospheric and emissivity corrections), which has not used in other previous studies based on Landsat imagery in the Cordillera Blanca (Silverio and Jaquet, 2005; Paul et al., 2004b; Burns and Nolin, 2014). This is useful for debris ice covered detection because the LST could be a few degrees higher than the clean ice covered at the moment of satellite data acquisition.

Glaciers in the southern part of the Cordillera Blanca lost a greater percentage of their area from 1987 to 2010 relative to the glaciers located in the northern part (Burns and Nolin, 2014). This study using Landsat/MSS, Landsat/TM, Landsat/ETM+, ASTER, IKONOS-2 and QuickBird identified 643.5 km^2 of glacierised area in 1987 and 482.4 km^2 in 2010, resulting in a total loss of 161 km^2 (25%). Direct comparison between our findings and those reported by Burns and Nolin could not be performed in this work since the study areas are different. However, the decrease in total glacier area from 1987 to 2010 in our study was −32.5%, whereas Burns and

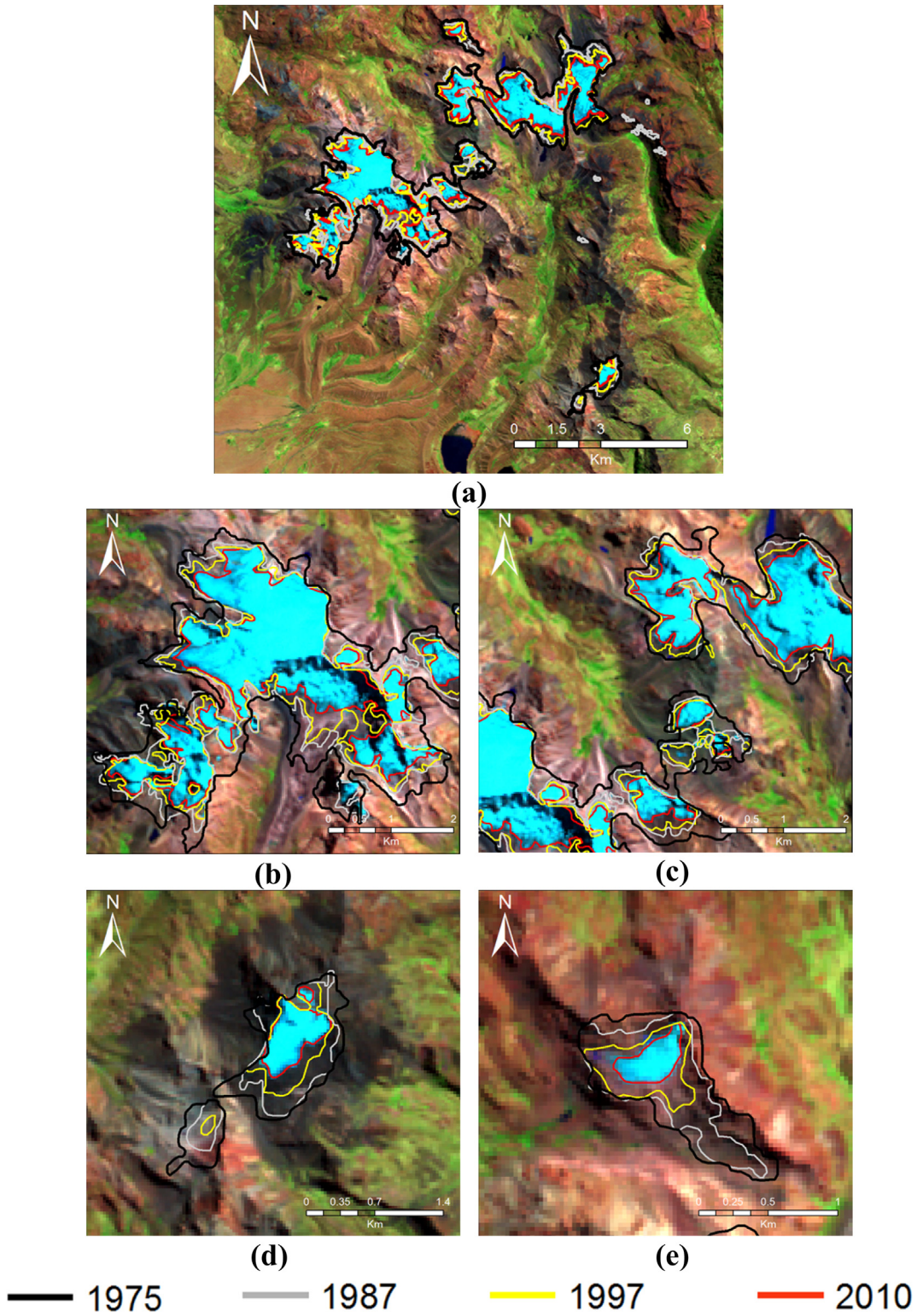

Fig. 5. Spatial patterns in clean ice glacier for the study area between 1975 and 2010. Black, grey, yellow and red lines indicate the estimated glacier limits for each year displayed over an Landsat-RGB (742) image acquired in 2010. (a) Nevados Caullaraju/Pastoruri and surrounded glaciers, (b) Caullaraju and Jenhuaracra, (c) Condorjitanca (d) Rajutuna and (e) Santon. Solid lines and dot lines are represented on the left Y axis and right Y axis respectively, to better representation of the smaller glaciers (<5 km^2 approx.). (For interpretation of the references to colour in this figure legend, the reader is referred to the web version of this article.)

Nolin (2014) found a decrease in the Pachacoto sub-watershed (located near our study area) for that period of around −37%, which seems to be consistent with our results. These trends are also comparable to the trend indicated by the ground-truth data, −3.3 km^2 per decade from 1970 to 2010 (or a decrease of −43% over the entire period). Regarding the Nevados Pastoruri/Tuco, an average loss of 1.4 km^2 per decade in terms of clean ice was identified, corresponding to a loss of 5.0 km^2 (−54%) from 1957 to

2010, 4.8 km^2 (−53%) from 1975 to 2010, and 3.1 km^2 (−42%) from 1987 to 2010. Analysis of a recent Landsat8/OLI image acquired in September 2013 also showed a decrease in clean ice area from 2010 to 2013 over Santon, Rajutuna and Pastoruri/Tuco Nevados (other Nevados were not analyzed because of the presence of clouds in the Landsat8 images), with a total loss of 0.03 km^2 (27%), 0.05 km^2 (14.7%), and 0.33 km^2 (7.6%), respectively, in only a three-year period. Other works about glaciers in the Cordillera Blanca, a comprehensive overview of the entire Cordillera Blanca using SPOT images and digitized maps retrieving was carried out by Georges (2004), which reveals an overall decline in glacierized area from 660 to 680 km^2 in 1970 to 620 km^2 in 1990, and slightly less than 600 km^2 at the end of the 20th century. However, Silverio and Jaquet (2005), in a similar study using Landsat TM data, detected 643 km^2 of glacierised area in 1987 and 600 km^2 in 1991. Therefore, the glaciated area analyzed was characterized differently in the different works and in turn, the total amount of glacier area was different. In this work, the glacier area was characterized based on spectral index.

6. Conclusions

Temporal evolution of clean ice and total glacier area (which includes both clean and debris-covered ice) over a group of Nevados was analyzed to extract the decreasing trends from 1975 to 2010, as well as from 1957 to 2010 over particular Nevados where an aerial photograph was available. Results showed a significant ($p < 0.05$) decreasing trend in both clean ice and total glacier area over the entire study area of around 4.5 km^2 per decade, leading to a total decrease of 15.9 km^2 in terms of clean ice area (−55%), or 22.5 km^2 in terms of total glacier area (−58%), in the last four decades.

The method has some drawbacks related to classification of dissimilar snow and ice types. The identification of seasonal snow in the study area is also a critical point for analyzing glacier area trends; although this drawback can be avoided in part by using imagery acquired in the dry season and local precipitation data. Uncertainties in the detection of debris-covered areas are also critical for correctly identifying the total glacier extent. Finally, this work provides an analysis of the current retreat of Cordillera Blanca glaciers by using long-term remote sensing imagery. These results can contribute to the development of future strategies in downstream runoff scenarios and to the design of new strategies for local adaptability of water resources management.

Acknowledgements

We acknowledge funding from the European Union (CEOP-AEGIS, project FP7-ENV-2007-1 Proposal No. 212921) and the Ministerio de Economía y Competitividad (EODIX, project AYA2008-0595-C04-01; CEOS-Spain, project AYA2011-29334-C02-01); U-Inicia VID-Uchile 4/0612 and Fondecyt-Initial 11130359. We thank the USGS for providing the Landsat imagery.

References

Andreassen, L., Paul, F., Kääb, A., Hausberg, J., 2008. Landsat-derived glacier inventory for Jotunheimen, Norway and deduced glacier changes since the 1930s. Cryosphere 2, 131–145.
Baldridge, A.M., Hook, S.J., Grove, C.I., Rivera, G., 2009. The ASTER spectral library version 2.0. Remote Sens. Environ. 113, 711–715.
Bolch, T., Menounos, B., Wheate, R., 2010. Landsat-based inventory of glaciers in western Canada, 1985-2005. Remote Sens. Environ. 114, 127–137.
Burns, P., Nolin, A., 2014. Using atmospherically-corrected Landsat imagery to measure glacier area change in the Cordillera Blanca, Peru from 1987 to 2010. Remote Sens. Environ. 140, 165–178.
Casey, K.A., Kääb, A., Benn, D.I., 2012. Geochemical characterization of supraglacial debris via in situ and optical remote sensing methods: a case study in Khumbu Himalaya, Nepal. Cryosphere 6, 85–100.
Chander, G., Markham, B., 2003. Revised Landsat-5 TM radiometric calibration procedures and postcalibration dynamic ranges. IEEE Trans. Geosci. Remote Sens. 41 (11), 2674–2677.
Chander, G., Markham, B.L., Barsi, J.A., 2007. Revised Landsat-5 thematic mapper radiometric calibration. IEEE Geosci. Remote Sens. Lett. 4 (3), 490–494.
Chander, G., Markham, B.L., Helder, D.L., 2009. Summary of current radiometric calibration coefficients for Landsat MSS, TM, ETM+, and EO-1 ALI sensors. Remote Sens. Environ. 113, 893–903.
Chavez, P.S., 1996. Image-based atmospheric correction – revisited and improved. Photogramm. Eng. Remote Sens. 62 (9), 1025–1036.
Dozier, J., 1989. Spectral signature of Alpine snow cover from the Landsat thematic mapper. Remote Sens. Environ. 28, 9–22.
Frey, H., Paul, F., Strozzi, T., 2012. Compilation of a glacier inventory for the western Himalayas from satellite data: methods, challenges and results. Remote Sens. Environ. 124, 8320843.
Georges, C., 2004. The 20th Century glacier fluctuations in the tropical Cordillera Blanca, Peru. Arct. Antarct. Alp. Res. 36 (1), 100–107.
Jiménez-Muñoz, J.C., Cristóbal, J., Sobrino, J.A., Sòria, G., Ninyerola, M., Pons, X., 2009. Revision of the single-channel algorithm for land surface temperature retrieval from Landsat thermal-infrared data. IEEE Trans. Geosci. Remote Sens. 47 (1), 339–349.
Jomelli, V., Favier, V., Rabatelc, A., Brunsteind, D., Hoffmanne, G., Francouf, B., 2009. Fluctuations of glaciers in the tropical Andes over the last millennium and palaeoclimatic implications: a review. Palaeogeogr. Palaeoclimatol. Palaeoecol. 281, 269–282.
Juen, I., Kaser, G., Georges, C., 2007. Modelling observed and future runoff from a glacierized tropical catchment (Cordillera Blanca, Perú). Glob. Planet. Change 59, 37–48.
Kaser, G., Osmaston, H., 2001. Tropical Glaciers. In: International Hydrology Series. Cambridge University Press, p. 228.
Kaser, G., Juen, I., Georges, C., Gómez, J., Tamayo, W., 2003. The impact of glaciers on the runoff and the reconstruction of mass balance history from hydrological data in the tropical Cordillera Blanca, Perú. J. Hydrol. 282, 130–144.
Kendall, M.G., 1975. Rank Correlation Methods, fourth ed. Charles Griffin, London.
Klein, A.G., Isacks, B.L., 1999. Spectral mixture analysis of Landsat thematic mapper images applied to the detection of the transient snowline on tropical Andean glaciers. Glob. Planet. Change 22 (1–4), 139–154.
López-Moreno, J.I., Fontaneda, S., Bazo, J., Revuelto, J., Azorín-Molina, C., Valero-Garcés, B., co-authors, 2014. Glob. Planet. Change 112, 1–11.
Paul, F., Kääb, A., Maisch, M., Kellenberger, T., Haeberli, W., 2002. The new remote-sensing-derived Swiss glacier inventory: I Methods. Ann. Og. Glaciaol. 34, 355–361.
Paul, F., Kääb, A., Maisch, M., Kellenberger, T., Haeberli, W., 2004a. Rapid disintegration of Alpine glaciers observed with satellite data. Geophys. Res. Lett. 31.
Paul, F., Huggel, C., Kääb, A., 2004b. Combining satellite multispectral image data and a digital elevation model for mapping debris-covered glaciers. Remote Sens. Environ. 89, 510–518.
Racoviteanu, A., Arnaud, Y., Williams, M., Ordonez, J., 2008a. Decadal changes in glacier parameters in the Cordillera Blanca, Peru, derived from remote sensing. J. Glaciaol. 54 (186), 499–510.
Racoviteanu, A.E., Williams, M.W., Barry, R.G., 2008b. Optical remote sensing of glacier characteristics: a review with focus on the Himalaya. Sensors 8, 3355–3383.
Racoviteanu, A., Williams, M., 2012. Decision tree and texture analysis for mapping debris-covered glaciers in the Kangchenjunga area, eastern Himalaya. Remote Sens. 4, 3078–3109.
Raup, B., Racoviteanu, A., Singh, S.J., Helm, C., Armstrong, R., Arnaud, Y., 2007. The GLIMS geospatial glacier database. A new tool for studying glacier change. Glob. Planet. Change 56 (1–2), 101–110.
Schauwecker, S., Rohrer, M., Acuña, D., Cochachin, A., Dávila, L., Frey, H., Giráldez, C., Gómez, J., Huggel, C., et al., 2014. Climate trends and glacier retreat in the Cordillera Blanca, Peru, revisited. Glob. Planet. Change 119, 85–97.
Sen, P.K., 1968. Estimates of the regression coefficient based on Kendall's tau. J. Am. Stat. Assoc. 63, 1379–1389.
Silverio, W., Jaquet, J.-M., 2005. Glacial cover mapping (1987-1996) of the Cordillera Blanca (Peru) using satellite imagery. Remote Sens. Environ. 95, 342–350.
Sobrino, J.A., Jiménez-Muñoz, J.C., Sòria, G., Romaguera, M., Guanter, L., Moreno, J., Plaza, A., Martínez, P., 2008. Land surface emissivity retrieval from different VNIR and TIR sensors. IEEE Trans. Geosci. Remote Sens. 46 (2), 316–327.
Solomina, O., Jomelli, V., Kaser, G., Ames, A., Berger, B., Pouyad, B., 2007. Lichenometry in the Cordillera Blanca, Peru: "Little Ice Age" moraine chronology. Glob. Planet. Change 59, 225–235.
Vuille, M., Francou, B., Wagnon, P., Juen, I., Kaser, G., Mark, B., Bradley, R., 2008a. Climate change and tropical andean glaciers: past, present and future. Earth-Sci. Rev. 89, 79–96.
Vuille, M., Kaser, G., Juen, I., 2008b. Glacier mass balance variability in the Cordillera Blanca, Peru and its relationship with climate and the large-scale circulation. Glob. Planet. Change 63, 14–28.
Yin, D., Cao, X., Chen, X., Shao, Y., Chen, J., 2013. Comparison of automatic thresholding methods for snow-cover mapping using Landsat TM imagery. Int. J. Remote Sens. 34 (19), 6529–6538.